第42卷第3期
2025 年 6 月

计 算 力 学 学 报
Chinese Journal of Computational Mechanics

Vol. 42, No. 3
June 2025

DOI:10.7511/jslx20240117002

基于薄板样条径向基函数的功能梯度板静力分析

宋薇薇*[1,2,3]， 项 松[1,2]， 赵 锐[1,2]

(1.沈阳航空航天大学 辽宁省通用航空重点实验室,沈阳 110136;
2.辽宁通用航空研究院,沈阳 110136;3.沈阳航空航天大学 民用航空学院,沈阳 110136)

摘 要:采用高阶剪切变形理论来对功能梯度板进行建模。控制微分方程采用基于薄板样条径向基函数的无网格方法离散。本文的计算结果与已有文献的计算结果进行了比较,两者具有较好的一致性,同时说明薄板样条径向基函数法在功能梯度板分析中的准确性和有效性。本文提出的考虑层边界离散性的新层合板理论比其他具有五个全局变量的层合板理论具有更精确的位移和应力。数值算例表明,采用薄板样条径向基函数对功能梯度板进行静力分析具有较高的精度和良好的收敛性。

关键词:薄板样条;径向基函数;功能梯度板;静力分析;高阶理论;无网格

中图分类号:O342 **文献标志码**:A **文章编号**:1007-4708(2025)03-0504-09

1 引 言

功能梯度材料(Functionally graded material)[1]指由两种或两种以上不同材料复合而成,且各组成成分的结构和性能在空间上沿着某一方向呈连续梯度变化的一种新型非匀质复合材料,可满足现代航天、航空、工业等高技术领域的特殊需要[2]。其可分为金属/合金、金属/非金属、非金属/陶瓷、金属/陶瓷、陶瓷/陶瓷等多种组合方式,因此可以获得多种特殊功能的材料。由于其新颖的材料可设计性思想和优良的结构性能,近年来引起国内外学者的广泛关注和研究[3]。

目前,许多学者研究了功能梯度板的静力特性。Li 等[4]提出了一种新的广义五变量剪切变形理论来计算功能梯度板的静力特性。其将具有形状参数 m 的小指数函数乘以经典三角剪切应变形状函数,以使横向剪切应变在功能梯度板的厚度方向上更准确地分布。Pandey 等[5]提出了一种高阶分层有限元公式,用于功能材料的静态和动态分析梯度材料夹层板。其使用混合规则(ROM)计算功能梯度板的有效材料特性。Rezaei 等[6]基于简单的一阶剪切变形板理论,研究了多孔功能梯度材料矩形板的自由振动分析。其利用变分法,导出了含孔隙 FG 板的运动控制方程。Kumar 等[7]提出了两种新的五变量高阶横向剪切变形理论,用于分析功能梯度材料板,同时,利用能量原理建立了 FGM 板的控制微分方程,实现了基于 Wendland 径向基函数的无网格离散 GDE 法。

基于径向基函数的无网格全局配置方法利用问题域中的所有节点近似求解偏微分方程。文献[8-10]已将其用于分析复合材料层合板的自由振动和静态变形。最常用的径向基函数包括复合二次径向基函数、逆复合二次径向基函数、高斯径向基函数和薄板样条径向基函数。在径向基函数近似中,形状参数对近似精度有重要影响。复合二次径向基函数、逆复合二次径向基函数和高斯径向基函数中形状参数的选择取决于支持域中的节点数和节点间距。与复合二次径向基函数、逆复合二次径向基函数和高斯径向基函数相比,薄板样条径向基函数中形状参数的选择简单而直接,只依赖于偏微分方程的最高阶数。

本文利用文献[11-16]的各种剪切变形理论和薄板样条径向基函数来研究功能梯度板的静力特性。通过将不同形状参数的计算结果与 Zenk-

收稿日期:2024-01-17; **修改稿收到日期**:2024-02-28.
基金项目:2022 年度辽宁省教育厅项目(LJKMZ 20220558;LJKMZ 20220564)资助.
作者简介:宋薇薇*(1983-),女,硕士,讲师(E-mail:214097295@qq.com).

引用本文:宋薇薇,项 松,赵 锐.基于薄板样条径向基函数的功能梯度板静力分析[J].计算力学学报,2025,**42**(3):504-512.
SONG Wei-wei,XIANG Song,ZHAO Rui. Static analysis of functionally graded plates based on thin plate spline radial basis function[J]. *Chinese Journal of Computational Mechanics*,2025,**42**(3):504-512.

our[17]的结果进行比较，来选择薄板样条径向基函数的形状参数。结果表明，当形状参数 $m=3$ 时，计算的结果最快收敛到 Zenkour[17]的解析解，两者具有较好的一致性。数值算例表明，采用薄板样条径向基函数对功能梯度板进行静力分析具有较高的精度和良好的收敛性。

2　控制方程和边界条件

x-y 平面与层合板的中平面重合，z 轴为沿板厚度的方向。该平面是具有长度 a 、宽度 b 和恒定厚度 h 的典型矩形板，其几何结构和坐标[18]如图 1 所示。

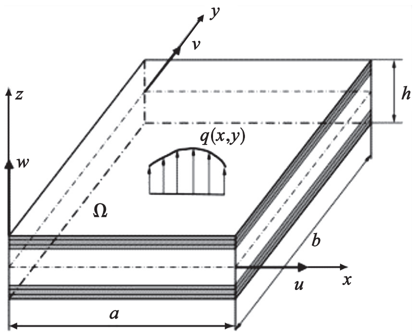

图 1　具有恒定厚度的复合材料层合板的几何结构和坐标

Fig. 1　Geometry and coordinates of a laminated composite plate with a constant thickness

高阶剪切变形理论的位移场[19]为

$$
\begin{aligned}
U &= u(x,y) - z\frac{\partial w(x,y)}{\partial x} + f(z)\phi_x(x,y) \\
V &= v(x,y) - z\frac{\partial w(x,y)}{\partial y} + f(z)\phi_y(x,y) \\
W &= w(x,y)
\end{aligned}
\tag{1}
$$

式中 u,v,w,ϕ_x,ϕ_y 为板的中平面的五个未知位移函数。$f(z)$ 是横向剪切函数，用于确定横向剪切应变和应力沿厚度的分布，列入表 1。

表 1　各种高阶层合板理论的横向剪切函数

Tab. 1　Lateral shear functions of various higher-order laminated plate theories

序号	理论方法	横向剪切函数
1	Ambartsumain[11]	$f(z)=\frac{z}{2}\left(\frac{1}{4}-\frac{z^2}{3h^2}\right)$
2	Aydogdu[12]	$f(z)=(z)(3)^{\frac{-2(z/h)^2}{\ln 3}}$
3	Karama 等[13]	$f(z)=ze^{-2(z/h)^2}$
4	Levinson[14]	$f(z)=z(1-\frac{4z^2}{3h^2})$
5	Shi[15]	$f(z)=\frac{5}{4}z\left(1-\frac{4z^2}{3h^2}\right)$
6	Soldatos[16]	$f(z)=\frac{h}{\pi}\sin\left(\frac{\pi z}{h}\right)$

板截面的翘曲以横向剪切函数为特征。不同横向剪切函数在板厚度上的分布如图 2(a)所示。此外，横向剪切应力在复合材料层合板的强度分析中起着非常重要的作用。层合板理论预测的层间横向剪切应力主要取决于与层合板理论中使用的横向剪切函数相关的横向剪切应变。各种横向剪切函数在板厚度上的导数如图 2(b)所示。从图 2 可以看出，Shi[15] 提出的横向剪切函数与 Levinson[14] 提出的横向剪切函数在板厚上的分布不同，尽管这两个横向剪切函数具有相似的多项式形式。

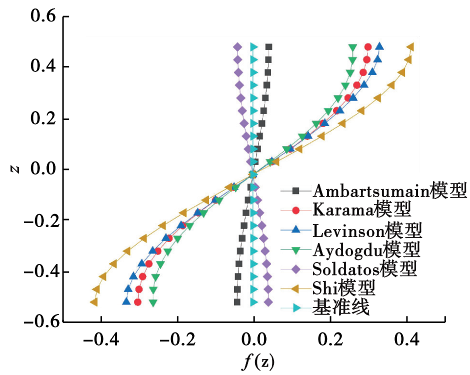

(a) 各种横向剪切函数沿板厚度的分布

(a) Distribution of various transverse shear functions along the plate thickness

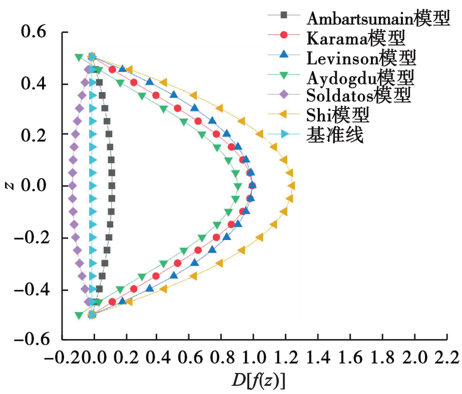

(b) 各种横向剪切函数沿厚度方向的导数

(b) Derivative of various transverse shear functions along the thickness direction

图 2　各种横向剪切函数沿板厚度的分布和各种横向剪切函数沿厚度方向的导数

Fig. 2　Distribution of various transverse shear functions along the plate thickness and derivative of various transverse shear functions along the thickness direction

应变-位移关系为

$$
\begin{Bmatrix} \varepsilon_x \\ \varepsilon_y \\ \gamma_{xy} \\ \gamma_{yz} \\ \gamma_{xz} \end{Bmatrix} = \begin{Bmatrix} \dfrac{\partial U}{\partial x} \\ \dfrac{\partial V}{\partial y} \\ \dfrac{\partial U}{\partial y}+\dfrac{\partial V}{\partial x} \\ \dfrac{\partial V}{\partial z}+\dfrac{\partial W}{\partial y} \\ \dfrac{\partial U}{\partial z}+\dfrac{\partial W}{\partial x} \end{Bmatrix}
\tag{2}
$$

通过将式(1)代入式(2),应变可表示为

$$
\begin{aligned}
&\varepsilon_x=\frac{\partial u}{\partial x}-z\frac{\partial^2 w}{\partial x^2}+f(z)\frac{\partial \phi_x}{\partial x}\\
&\varepsilon_y=\frac{\partial v}{\partial y}-z\frac{\partial^2 w}{\partial y^2}+f(z)\frac{\partial \phi_y}{\partial y}\\
&\gamma_{xy}=\frac{\partial u}{\partial y}+\frac{\partial v}{\partial x}-2z\frac{\partial^2 w}{\partial x\partial y}+f(z)\left(\frac{\partial \phi_x}{\partial y}+\frac{\partial \phi_y}{\partial x}\right)\\
&\gamma_{yz}=\frac{\partial f(z)}{\partial z}\phi_y\\
&\gamma_{xz}=\frac{\partial f(z)}{\partial z}\phi_x
\end{aligned}
\tag{3}
$$

功能梯度板在全局 x-y-z 坐标系中的应力-应变关系可以写为

$$
\begin{Bmatrix}\sigma_{xx}\\ \sigma_{yy}\\ \tau_{xy}\\ \tau_{yz}\\ \tau_{zx}\end{Bmatrix}=\begin{bmatrix}Q_{11}&Q_{12}&0&0&0\\ Q_{12}&Q_{11}&0&0&0\\ 0&0&Q_{66}&0&0\\ 0&0&0&Q_{44}&0\\ 0&0&0&0&Q_{55}\end{bmatrix}\begin{Bmatrix}\varepsilon_x\\ \varepsilon_y\\ \gamma_{xy}\\ \gamma_{yz}\\ \gamma_{zx}\end{Bmatrix}
\tag{4}
$$

其中

$$
\begin{aligned}
&Q_{11}=\frac{E(z)}{1-v^2}\\
&Q_{12}=\frac{vE(z)}{1-v^2}\\
&Q_{66}=Q_{44}=Q_{55}=\frac{E(z)}{2(1+v)}\\
&E(z)=(E_c-E_m)\left(\frac{1}{2}+\frac{z}{h}\right)^p+E_m
\end{aligned}
\tag{5}
$$

式中 E_c 和 E_m 分别表示陶瓷和金属的弹性模量,p 为幂律指数,z 是从中间平面开始量取的距离,h 是板的厚度。从式(5)可以看出,$E(z)=E_c$ 在上表面 $z/h=0.5$,$E(z)=E_m$ 在下表面 $z/h=-0.5$。功能梯度板的上表面为纯陶瓷,下表面为纯金属。

控制方程由虚功率原理推导而来。

$$
\delta V_\varepsilon=\delta V_q \tag{6}
$$

虚应变能可以表示为

$$
\delta V_\varepsilon=\iiint(\sigma_x\delta\varepsilon_x+\sigma_y\delta\varepsilon_y+\tau_{xy}\delta\gamma_{xy}+\tau_{zx}\delta\gamma_{zx}+\tau_{yz}\delta\gamma_{yz})\mathrm{d}x\mathrm{d}y\mathrm{d}z \tag{7}
$$

作用力所做的虚功可以表示为

$$
\delta V_q=\iint q\delta w\,\mathrm{d}x\mathrm{d}y \tag{8}
$$

通过将式(7,8)代入式(6),可得

$$
\iiint(\sigma_x\delta\varepsilon_x+\sigma_y\delta\varepsilon_y+\tau_{xy}\delta\gamma_{xy}+\tau_{zx}\delta\gamma_{zx}+\tau_{yz}\delta\gamma_{yz})\mathrm{d}x\mathrm{d}y\mathrm{d}z=\iint q\delta w\,\mathrm{d}x\mathrm{d}y \tag{9}
$$

通过将式(4)代入式(9),可得

$$
\begin{aligned}
&\frac{\partial N_x}{\partial x}+\frac{\partial N_{xy}}{\partial y}=0\\
&\frac{\partial N_y}{\partial y}+\frac{\partial N_{xy}}{\partial x}=0\\
&\frac{\partial^2 M_x}{\partial x^2}+\frac{\partial^2 M_y}{\partial y^2}+2\frac{\partial^2 M_{xy}}{\partial x\partial y}=q\\
&\frac{\partial M_x^f}{\partial x}+\frac{\partial M_{xy}^f}{\partial y}-Q_x^f=0\\
&\frac{\partial M_y^f}{\partial y}+\frac{\partial M_{xy}^f}{\partial x}-Q_y^f=0
\end{aligned}
\tag{10}
$$

其中

$$
\begin{aligned}
&N_x=A_{11}\frac{\partial u}{\partial x}+A_{12}\frac{\partial v}{\partial y}-B_{11}\frac{\partial^2 w}{\partial x^2}-B_{12}\frac{\partial^2 w}{\partial y^2}+E_{11}\frac{\partial \phi_x}{\partial x}+E_{12}\frac{\partial \phi_y}{\partial y}\\
&N_y=A_{12}\frac{\partial u}{\partial x}+A_{11}\frac{\partial v}{\partial y}-B_{12}\frac{\partial^2 w}{\partial x^2}-B_{11}\frac{\partial^2 w}{\partial y^2}+E_{12}\frac{\partial \phi_x}{\partial x}+E_{11}\frac{\partial \phi_y}{\partial y}\\
&N_{xy}=A_{66}\left(\frac{\partial u}{\partial y}+\frac{\partial v}{\partial x}\right)-2B_{66}\frac{\partial^2 w}{\partial x\partial y}+E_{66}\left(\frac{\partial \phi_x}{\partial y}+\frac{\partial \phi_y}{\partial x}\right)\\
&M_x=B_{11}\frac{\partial u}{\partial x}+B_{12}\frac{\partial v}{\partial y}-D_{11}\frac{\partial^2 w}{\partial x^2}-D_{12}\frac{\partial^2 w}{\partial y^2}+F_{11}\frac{\partial \phi_x}{\partial x}+F_{12}\frac{\partial \phi_y}{\partial y}\\
&M_y=B_{12}\frac{\partial u}{\partial x}+B_{11}\frac{\partial v}{\partial y}-D_{12}\frac{\partial^2 w}{\partial x^2}-D_{11}\frac{\partial^2 w}{\partial y^2}+F_{12}\frac{\partial \phi_x}{\partial x}+F_{11}\frac{\partial \phi_y}{\partial y}\\
&M_{xy}=B_{66}\left(\frac{\partial u}{\partial y}+\frac{\partial v}{\partial x}\right)-2D_{66}\frac{\partial^2 w}{\partial x\partial y}+F_{66}\left(\frac{\partial \phi_x}{\partial y}+\frac{\partial \phi_y}{\partial x}\right)\\
&M_x^f=E_{11}\frac{\partial u}{\partial x}+E_{12}\frac{\partial v}{\partial y}-F_{11}\frac{\partial^2 w}{\partial x^2}-F_{12}\frac{\partial^2 w}{\partial y^2}+H_{11}\frac{\partial \phi_x}{\partial x}+H_{12}\frac{\partial \phi_y}{\partial y}\\
&M_y^f=E_{12}\frac{\partial u}{\partial x}+E_{11}\frac{\partial v}{\partial y}-F_{12}\frac{\partial^2 w}{\partial x^2}-F_{11}\frac{\partial^2 w}{\partial y^2}+H_{12}\frac{\partial \phi_x}{\partial x}+H_{11}\frac{\partial \phi_y}{\partial y}\\
&M_{xy}^f=E_{66}\left(\frac{\partial u}{\partial y}+\frac{\partial v}{\partial x}\right)-2F_{66}\frac{\partial^2 w}{\partial x\partial y}+H_{66}\left(\frac{\partial \phi_x}{\partial y}+\frac{\partial \phi_y}{\partial x}\right)
\end{aligned}
\tag{11}
$$

$$
Q_y^f=A_{44}\phi_y,\quad Q_x^f=A_{55}\phi_x
$$

$$
A_{ij}=\int_{-\frac{h}{2}}^{\frac{h}{2}}Q_{ij}\,\mathrm{d}z,\ B_{ij}=\int_{-\frac{h}{2}}^{\frac{h}{2}}Q_{ij}z\,\mathrm{d}z
$$

$$
D_{ij}=\int_{-\frac{h}{2}}^{\frac{h}{2}}Q_{ij}z^2\,\mathrm{d}z,\ E_{ij}=\int_{-\frac{h}{2}}^{\frac{h}{2}}Q_{ij}f(z)\,\mathrm{d}z
$$

$$F_{ij}=\int_{-\frac{h}{2}}^{\frac{h}{2}}Q_{ij}zf(z)\mathrm{d}z \quad (i,j=1,2,6)$$
$$H_{ij}=\int_{-\frac{h}{2}}^{\frac{h}{2}}Q_{ij}f^2(z)\mathrm{d}z$$
$$A_{ij}=\int_{-\frac{h}{2}}^{\frac{h}{2}}Q_{ij}\left(\frac{\partial f(z)}{\partial z}\right)^2\mathrm{d}z \quad (i,j=4,5) \qquad (12)$$

通过将式(11)代入式(10)可得位移方面的控制方程为

$$A_{11}\frac{\partial^2 u}{\partial x^2}+A_{12}\frac{\partial^2 v}{\partial x\partial y}-B_{11}\frac{\partial^3 w}{\partial x^3}-B_{12}\frac{\partial^3 w}{\partial x\partial y^2}+E_{11}\frac{\partial^2 \phi_x}{\partial x^2}+E_{12}\frac{\partial^2 \phi_y}{\partial x\partial y}+A_{66}\left(\frac{\partial^2 u}{\partial y^2}+\frac{\partial^2 v}{\partial x\partial y}\right)-2B_{66}\frac{\partial^3 w}{\partial x\partial y^2}+E_{66}\left(\frac{\partial^2 \phi_x}{\partial y^2}+\frac{\partial^2 \phi_y}{\partial x\partial y}\right)=0$$

$$A_{12}\frac{\partial^2 u}{\partial x\partial y}+A_{11}\frac{\partial^2 v}{\partial y^2}-B_{12}\frac{\partial^3 w}{\partial x^2\partial y}-B_{11}\frac{\partial^3 w}{\partial y^3}+E_{12}\frac{\partial^2 \phi_x}{\partial x\partial y}+E_{11}\frac{\partial^2 \phi_y}{\partial y^2}+A_{66}\left(\frac{\partial^2 u}{\partial x\partial y}+\frac{\partial^2 v}{\partial x^2}\right)-2B_{66}\frac{\partial^3 w}{\partial x^2\partial y}+E_{66}\left(\frac{\partial^2 \phi_x}{\partial x\partial y}+\frac{\partial^2 \phi_y}{\partial x^2}\right)=0 \qquad (13a)$$

$$B_{11}\frac{\partial^3 u}{\partial x^3}+B_{12}\frac{\partial^3 v}{\partial x^2\partial y}-D_{11}\frac{\partial^4 w}{\partial x^4}-D_{12}\frac{\partial^4 w}{\partial x^2\partial y^2}+F_{11}\frac{\partial^3 \phi_x}{\partial x^3}+F_{12}\frac{\partial^3 \phi_y}{\partial x^2\partial y}+B_{12}\frac{\partial^3 u}{\partial x\partial y^2}+B_{11}\frac{\partial^3 v}{\partial y^3}-D_{12}\frac{\partial^4 w}{\partial x^2\partial y^2}-D_{11}\frac{\partial^4 w}{\partial y^4}+F_{12}\frac{\partial^3 \phi_x}{\partial x\partial y^2}+F_{11}\frac{\partial^3 \phi_y}{\partial y^3}+2B_{66}\left(\frac{\partial^3 u}{\partial x\partial y^2}+\frac{\partial^3 v}{\partial x^2\partial y}\right)-4D_{66}\frac{\partial^4 w}{\partial x^2\partial y^2}+2F_{66}\left(\frac{\partial^3 \phi_x}{\partial x\partial y^2}+\frac{\partial^3 \phi_y}{\partial x^2\partial y}\right)=q$$

$$E_{11}\frac{\partial^2 u}{\partial x^2}+E_{12}\frac{\partial^2 v}{\partial x\partial y}-F_{11}\frac{\partial^3 w}{\partial x^3}-F_{12}\frac{\partial^3 w}{\partial x\partial y^2}+H_{11}\frac{\partial^2 \phi_x}{\partial x^2}+H_{12}\frac{\partial^2 \phi_y}{\partial x\partial y}+E_{66}\left(\frac{\partial^2 u}{\partial y^2}+\frac{\partial^2 v}{\partial x\partial y}\right)-2F_{66}\frac{\partial^3 w}{\partial x\partial y^2}+H_{66}\left(\frac{\partial^2 \phi_x}{\partial y^2}+\frac{\partial^2 \phi_y}{\partial x\partial y}\right)-A_{55}\phi_x=0$$

$$E_{12}\frac{\partial^2 u}{\partial x\partial y}+E_{11}\frac{\partial^2 v}{\partial y^2}-F_{12}\frac{\partial^3 w}{\partial x^2\partial y}-F_{11}\frac{\partial^3 w}{\partial y^3}+H_{12}\frac{\partial^2 \phi_x}{\partial x\partial y}+H_{11}\frac{\partial^2 \phi_y}{\partial y^2}+E_{66}\left(\frac{\partial^2 u}{\partial x\partial y}+\frac{\partial^2 v}{\partial x^2}\right)-2F_{66}\frac{\partial^3 w}{\partial x^2\partial y}+H_{66}\left(\frac{\partial^2 \phi_x}{\partial x\partial y}+\frac{\partial^2 \phi_y}{\partial x^2}\right)-A_{44}\phi_y=0 \qquad (13b)$$

简支边的边界条件为

$$x=0,a:v=0,\phi_y=0,w=0,M_x=0,N_x=0$$
$$y=0,b:u=0,\phi_x=0,w=0,M_y=0,N_y=0 \qquad (14)$$

3 控制方程和边界条件的离散化

式(13)的解可近似为

$$u=\sum_{j=1}^{N}\alpha_j^u g(\|X-X_j\|)$$
$$v=\sum_{j=1}^{N}\alpha_j^v g(\|X-X_j\|)$$
$$w=\sum_{j=1}^{N}\alpha_j^w g(\|X-X_j\|)$$
$$\phi_x=\sum_{j=1}^{N}\alpha_j^{\phi_x} g(\|X-X_j\|)$$
$$\phi_y=\sum_{j=1}^{N}\alpha_j^{\phi_y} g(\|X-X_j\|). \qquad (15)$$

其中 N 是节点总数，α_j^u，α_j^v，α_j^w，$\alpha_j^{\phi_x}$，$\alpha_j^{\phi_y}$ 是 5 N 未知系数，$g(\|X-X_j\|)$ 是径向基函数，$\|X-X_j\|$ 是节点 X 和节点 X_j 之间的距离。本文使用的函数是薄板样条径向基函数

$$g_j=r_{ij}^{2m}\log(r_{ij}) \quad (m=2,3,4,\cdots) \qquad (16)$$

式中 $r_{ij}=\sqrt{(x_i-x_j)^2+(y_i-y_j)^2}$ 表示节点 (x_i,y_i) 和节点 (x_j,y_j) 之间的距离，m 是形状参数。

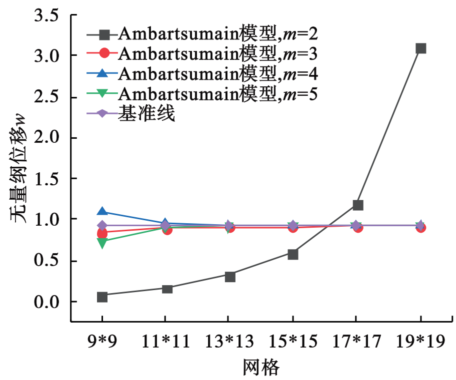

图 3 通过各种网格分布和形状参数 m（Ambartsumain 模型）计算简支方形功能梯度板（$a/h=10$，$p=1$）的无量纲位移 w

Fig. 3 Nondimensional displacements w of a simply square functionallygraded plate($a/h=10$, $p=1$)calculated by the various grid distribution and shape parameter m (Ambartsumain model)

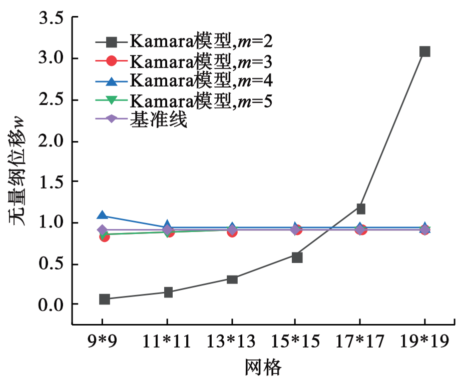

图 4 由各种网格分布和形状参数 m（Karama 模型）计算的简支功能梯度方形板（$a/h=10$，$p=1$）的无量纲位移 w

Fig. 4 Nondimensional displacements w of a simply square functionally graded plate($a/h=10$, $p=1$)calculated by the various grid distribution and shape parameter m (Karama model)

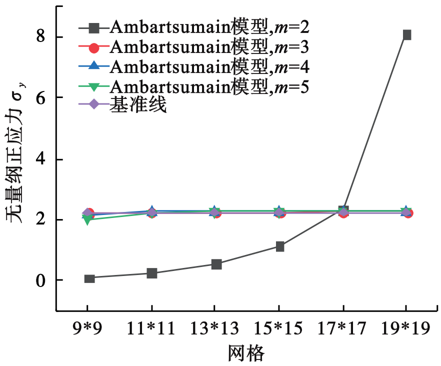

图 5 Ambartsumain 模型简支功能梯度方形板的无量纲正应力 σ_y ($a/h=10$, $p=1$)

Fig. 5 Nondimensional normal stress σ_y of a simply square functionally graded plate($a/h=10$, $p=1$) calculated by the various grid distribution and shape parameter m (Ambartsumain model)

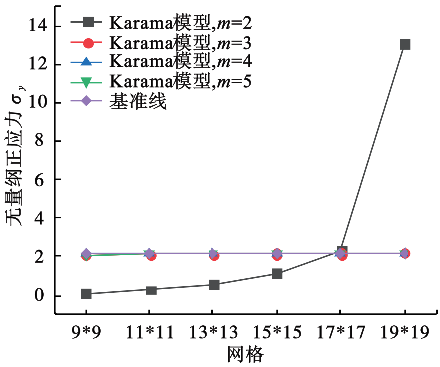

图 6 Karama 模型简支功能梯度方形板的无量纲正应力 σ_y ($a/h=10$, $p=1$)

Fig. 6 Nondimensional normal stress σ_y of a simply square functionally graded plate($a/h=10$, $p=1$) calculated by the various grid distribution and shape parameter m (Karama model)

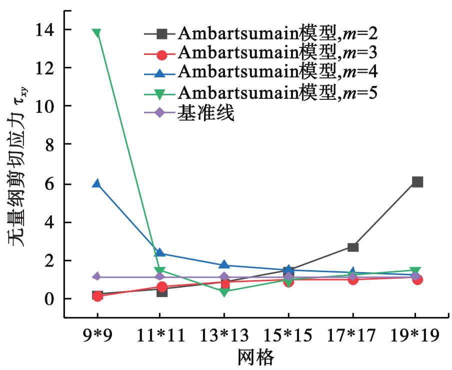

图 7 Ambartsumain 模型简支方形功能梯度板的无量纲剪切应力 τ_{xy} ($a/h=10$, $p=1$)

Fig. 7 Nondimensional transverse shear stress τ_{xy} of a simply square functionally graded plate($a/h=10$, $p=1$) calculated by the various grid distribution and shape parameter m (Ambartsumain model)

径向基函数中的形状参数对近似精度起着重要作用。薄板样条径向基函数的形状参数的选择比复合二次径向基函数、逆复合二次径向基函数和高斯径向基函数的形状参数的选择更加容易，但薄板样条径向基函数在节点间距为零时存在奇异性的缺点。为了消除薄板样条径向基函数的奇异性，当两个节点之间的距离为零时，$r_{ij}^2=r_{ij}^2+\zeta$。本文的无穷小值 $\zeta=1\times10^{-30}$。通过数值实验，得到了无穷小的数值解。当无穷小值小于 1×10^{-30} 时，无法得到结果。

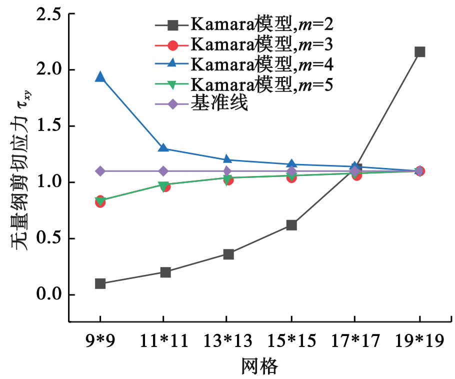

图 8 Karama 模型简支方形功能梯度板的无量纲剪切剪应力 τ_{xy} ($a/h=10$, $p=1$)

Fig. 8 Nondimensional transverse shear stress τ_{xy} of a simply square functionally graded plate($a/h=10$, $p=1$) calculated by the various grid distribution and shape parameter m (Karama model)

将式(15)代入式(13a)，可得离散化控制方程为

$$
\begin{aligned}
&\sum_{j=1}^{N}\alpha_j^u\left(A_{11}\frac{\partial^2 g}{\partial x^2}+A_{66}\frac{\partial^2 g}{\partial y^2}\right)+\\
&\sum_{j=1}^{N}\alpha_j^v\left(A_{12}\frac{\partial^2 g}{\partial x\partial y}+A_{66}\frac{\partial^2 g}{\partial x\partial y}\right)+\\
&\sum_{j=1}^{N}\alpha_j^w\left(-B_{11}\frac{\partial^3 g}{\partial x^3}-(B_{12}+2B_{66})\frac{\partial^3 g}{\partial x\partial y^2}\right)+\\
&\sum_{j=1}^{N}\alpha_j^{\phi_x}\left(E_{11}\frac{\partial^2 g}{\partial x^2}+E_{66}\frac{\partial^2 g}{\partial y^2}\right)+\\
&\sum_{j=1}^{N}\alpha_j^{\phi_y}(E_{12}+E_{66})\frac{\partial^2 g}{\partial x\partial y}=0
\end{aligned}
\tag{17}
$$

方程(13b)和边界条件可以用同样的方式离散。离散化的控制方程和边界条件可以表示为

$$
\begin{bmatrix} Lg \\ Bg \end{bmatrix}\{\alpha\}=\begin{bmatrix} q \\ 0 \end{bmatrix} \tag{18}
$$

推导可得

$$
\alpha=\begin{bmatrix} Lg \\ Bg \end{bmatrix}^{-1}\begin{bmatrix} q \\ 0 \end{bmatrix} \tag{19}
$$

位移可通过将式(19)代入式(15)的第三个公式来计算，应力可通过式(4)获得。

表 2 简支方形功能梯度板的无量纲应力和位移($a/h=10$，$p=1\sim10$)

Tab.2 Dimensionless stress and displacement of a simply supported square functionally graded plate ($a/h=10$，$p=1\sim10$)

p	方法	$\bar{w}$	$\bar{\sigma}_x$	$\bar{\sigma}_y$	$\bar{\tau}_{yz}$	$\bar{\tau}_{xz}$	$\bar{\tau}_{xy}$
1	Zenkour[17]	0.9287	4.4745	2.1692	0.5446	0.5114	1.1143
	本文(Amb)	0.9206	4.5815	2.2613	0.4889	0.4585	1.0091
	本文(Kar)	0.9206	4.4567	2.1668	0.4889	0.4585	1.0766
	本文(Lev)	0.9206	4.4423	2.1598	0.4889	0.4585	1.0816
	本文(Ayd)	0.9206	4.4760	2.1787	0.4889	0.4585	1.0681
	本文(Sol)	0.9206	4.3869	2.1535	0.4889	0.4585	1.0862
	本文(Shi)	0.9206	4.4026	2.1309	0.4889	0.4585	1.1024
2	Zenkour[17]	1.1940	5.2296	2.0338	0.5734	0.4700	0.9907
	本文(Amb)	1.1826	5.3835	2.1488	0.5150	0.4193	0.9058
	本文(Kar)	1.1826	5.2124	2.0346	0.5150	0.4193	0.9614
	本文(Lev)	1.1826	5.1928	2.0262	0.5150	0.4193	0.9655
	本文(Ayd)	1.1826	5.2389	2.0491	0.5150	0.4193	0.9544
	本文(Sol)	1.1826	5.1169	2.0185	0.5150	0.4193	0.9692
	本文(Shi)	1.1826	5.1383	1.9912	0.5150	0.4193	0.9825
3	Zenkour[17]	1.3200	5.6108	1.8593	0.5629	0.4367	1.0047
	本文(Amb)	1.3070	5.8100	1.9874	0.5076	0.3919	0.9275
	本文(Kar)	1.3070	5.5908	1.8616	0.5076	0.3919	0.9768
	本文(Lev)	1.3070	5.5656	1.8523	0.5076	0.3919	0.9805
	本文(Ayd)	1.3070	5.6247	1.8775	0.5076	0.3919	0.9706
	本文(Sol)	1.3070	5.4684	1.8438	0.5076	0.3919	0.9838
	本文(Shi)	1.3070	5.4958	1.8137	0.5076	0.3919	0.9956
4	Zenkour[17]	1.3890	5.8915	1.7197	0.5346	0.4204	1.0298
	本文(Amb)	1.3752	6.1294	1.8522	0.4885	0.3798	0.9585
	本文(Kar)	1.3752	5.8735	1.7226	0.4885	0.3798	1.0029
	本文(Lev)	1.3752	5.8441	1.7130	0.4885	0.3798	1.0062
	本文(Ayd)	1.3752	5.9131	1.7390	0.4885	0.3798	0.9973
	本文(Sol)	1.3752	5.7305	1.7043	0.4885	0.3798	1.0092
	本文(Shi)	1.3752	5.7626	1.6733	0.4885	0.3798	1.0198
5	Zenkour[17]	1.4356	6.1504	1.6104	0.5031	0.4177	1.0451
	本文(Amb)	1.4215	6.4182	1.7416	0.4599	0.3796	0.9785
	本文(Kar)	1.4215	6.1330	1.6137	0.4599	0.3796	1.0182
	本文(Lev)	1.4215	6.1003	1.6043	0.4599	0.3796	1.0211
	本文(Ayd)	1.4215	6.1772	1.6299	0.4599	0.3796	1.0132
	本文(Sol)	1.4215	5.9737	1.5957	0.4599	0.3796	1.0238
	本文(Shi)	1.4215	6.0094	1.5651	0.4599	0.3796	1.0333
6	Zenkour[17]	1.4727	6.4043	1.5214	0.4755	0.4227	1.0536
	本文(Amb)	1.4584	6.6954	1.6477	0.4397	0.3860	0.9903
	本文(Kar)	1.4584	6.3881	1.5242	0.4397	0.3860	1.0265
	本文(Lev)	1.4584	6.3528	1.5151	0.4397	0.3860	1.0291
	本文(Ayd)	1.4584	6.4357	1.5398	0.4397	0.3860	1.0219
	本文(Sol)	1.4584	6.2165	1.5068	0.4397	0.3860	1.0316
	本文(Shi)	1.4584	6.2549	1.4772	0.4397	0.3860	1.0402
7	Zenkour[17]	1.5049	6.6547	1.4467	0.4543	0.4310	1.0589
	本文(Amb)	1.4905	6.9627	1.5663	0.4194	0.3952	0.9980
	本文(Kar)	1.4905	6.6375	1.4490	0.4194	0.3952	1.0319
	本文(Lev)	1.4905	6.6001	1.4404	0.4194	0.3952	1.0344
	本文(Ayd)	1.4905	6.6879	1.4638	0.4194	0.3952	1.0276
	本文(Sol)	1.4905	6.4559	1.4324	0.4194	0.3952	1.0367
	本文(Shi)	1.4905	6.4965	1.4044	0.4194	0.3952	1.0448
8	Zenkour[17]	1.5343	6.8999	1.3829	0.4392	0.4399	1.0628
	本文(Amb)	1.5198	7.2205	1.4954	0.4074	0.4048	1.0034
	本文(Kar)	1.5198	6.8907	1.3855	0.4074	0.4048	1.0364
	本文(Lev)	1.5198	6.8527	1.3774	0.4074	0.4048	1.0388
	本文(Ayd)	1.5198	6.9417	1.3994	0.4074	0.4048	1.0322
	本文(Sol)	1.5198	6.7064	1.3700	0.4074	0.4048	1.0411
	本文(Shi)	1.5198	6.7477	1.3437	0.4074	0.4048	1.0490
9	Zenkour[17]	1.5617	7.1383	1.3283	0.4291	0.4481	1.0662
	本文(Amb)	1.5472	7.4673	1.4339	0.4004	0.4137	1.0073
	本文(Kar)	1.5472	7.1257	1.3303	0.4004	0.4137	1.0393
	本文(Lev)	1.5472	7.0864	1.3226	0.4004	0.4137	1.0416
	本文(Ayd)	1.5472	7.1786	1.3434	0.4004	0.4137	1.0352
	本文(Sol)	1.5472	6.9349	1.3156	0.4004	0.4137	1.0438
	本文(Shi)	1.5472	6.9776	1.2909	0.4004	0.4137	1.0515
10	Zenkour[17]	1.5876	7.3689	1.2820	0.4227	0.4552	1.0694
	本文(Amb)	1.5730	7.7028	1.3810	0.3972	0.4210	1.0102
	本文(Kar)	1.5730	7.3483	1.2828	0.3972	0.4210	1.0419
	本文(Lev)	1.5730	7.3076	1.2756	0.3972	0.4210	1.0443
	本文(Ayd)	1.5730	7.4032	1.2952	0.3972	0.4210	1.0379
	本文(Sol)	1.5730	7.1503	1.2689	0.3972	0.4210	1.0464
	本文(Shi)	1.5730	7.1946	1.2454	0.3972	0.4210	1.0540

注：Ambartsumain 简写为 Amb；Karama 简写为 Kar；Levinson 简写为 Lev；Aydogdu 简写为 Ayd；Soldatos 简写为 Sol。

4 数值算例

考虑均布荷载下 $a/h=10$ 的简支方形功能梯度板。功能梯度板由陶瓷和金属组成。陶瓷和金属的材料特性如下：

陶瓷：$E_c = 380$ GPa，$v = 0.3$

金属：$E_m = 70$ GPa，$v = 0.3$

根据式(5)，功能梯度材料的杨氏模量随板的厚度而变化。功能梯度材料的泊松比在整个板的厚度范围内是恒定的。

横向位移、正应力、面内剪切应力和横向剪切应力以归一化形式表示。

$$\bar{w} = \frac{10h^3 E_c w(a/2,a/2)}{q_0 a^4},\quad \bar{\sigma}_x = \frac{\sigma_x(a/2,a/2,h/2)h}{q_0 a}$$

$$\bar{\sigma}_y = \frac{\sigma_y(a/2,a/2,h/3)h}{q_0 a},\quad \bar{\tau}_{xy} = \frac{\tau_{xy}(0,0,-h/3)h}{q_0 a}$$

$$\bar{\tau}_{yz} = \frac{\tau_{yz}(a/2,0,h/6)h}{q_0 a},\quad \bar{\tau}_{xz} = \frac{\tau_{xz}(0,a/2,0)h}{q_0 a}$$

以 $a/h = 10$，$p = 1$ 的功能梯度四边形板为例，研究了本方法的收敛特性和形状参数的选择。由 Ambartsumain 模型和 Karama 模型计算的无量纲位移 w 如图 3 和图 4 所示。由 Ambartsumain 模型和 Karama 模型计算的无量纲正应力 σ_y 如图 5 和图 6 所示。由 Ambartsumain 模型和 Karama 模型计算的无量纲剪切应力 τ_{xy} 分别如图 7 和图 8 所

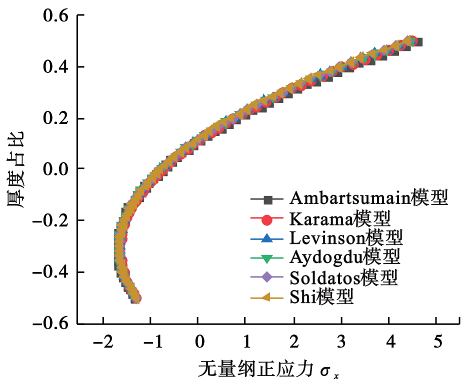

图 9　沿着简支方形功能梯度板的厚度方向获得无量纲正应力 σ_x（$p = 1, a/h = 10$）

Fig. 9　Nondimensional normal stress σ_x through the thickness of a simply supported square functionally graded plate（$p = 1, a/h = 10$）

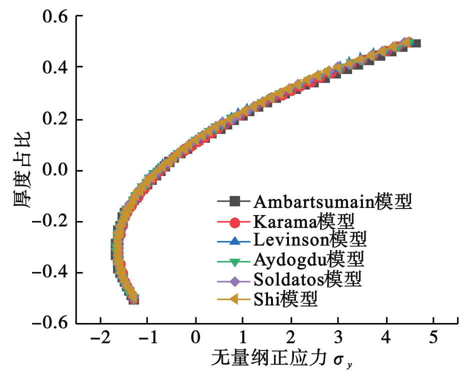

图 10　沿着简支方形功能梯度板的厚度方向获得无量纲正应力 σ_y（$p = 1, a/h = 10$）

Fig. 10　Nondimensional normal stress σ_y through the thickness of a simply supported square functionally graded plate（$p = 1, a/h = 10$）

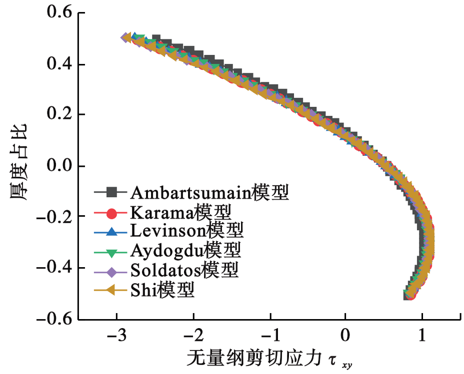

图 11　沿着简支方形功能梯度板的厚度方向获得无量纲剪切应力 τ_{xy}（$p = 1, a/h = 10$）

Fig. 11　Nondimensional shear stress τ_{xy} through the thickness of a simply supported square functionally graded plate（$p = 1, a/h = 10$）

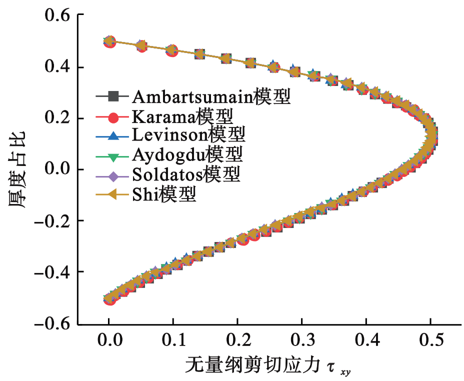

图 12　沿着简支方形功能梯度板的厚度方向获得无量纲剪切应力 τ_{xz}（$p = 1, a/h = 10$）

Fig. 12　Nondimensional shear stress τ_{xz} through the thickness of a simply supported square functionally graded plate（$p = 1, a/h = 10$）

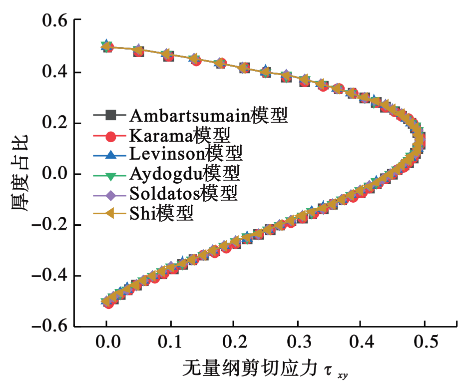

图 13　通过简支方形功能梯度板的厚度获得无量纲剪切应力 τ_{yz}（$p = 1, a/h = 10$）

Fig. 13　Nondimensional shear stress τ_{yz} through the thickness of a simply supported square functionally graded plate（$p = 1, a/h = 10$）

示。根据图 3～图 8，目前使用形状参数 $m = 3$ 计算的结果很快收敛到 Zenkour[17] 的解析解。文献[8-10]已经采用了形状参数 $m = 3$。在后面的部分中，使用了形状参数 $m = 3$ 和节点分布 17×17。

在研究了本方法的收敛特性和形状参数的选

择后，将各种剪切变形理论计算的结果与 Zenkour[17]的解析解进行了比较。表 2 列出了简支方形功能梯度板（ $a/h=10$ ，$p=1\sim10$ ）的无量纲应力和位移。可以发现，目前的结果与 Zenkour[17]的结果一致，位移和正应力的精度高于剪切应力的精度。

图 9～图 13 显示了通过简支方形功能梯度板厚度的无量纲应力（ $p=1, a/h=10$ ）。根据图 9～图 11，各种剪切变形理论产生紧密的面内剪切应力和正应力结果。从图 12 和图 13 可以看出各种剪切变形理论之间的剪切应力存在显著差异。

5　结　论

本文依据文献[11-16]提出了基于薄板样条径向基函数的无网格方法离散的各种剪切变形理论，以分析功能梯度板的静力特性。结果表明，薄板样条径向基函数法在功能梯度板分析中具有较高的精度。

参考文献（References）：

[1] 邓先琪，苏　成，马海涛．功能梯度梁静力与动力分析的格林函数法[J]．工程力学，2020，**37**(9)：248-256．(DENG Xian-qi，SU Cheng，MA Hai-tao．Green's function method for static and dynamic analysis of functionally graded beams[J]．*Engineering Mechanics*，2020，**37**(9)：248-256．(in Chinese))

[2] 杨正光，仲　政，戴　瑛．功能梯度矩形板的三维弹性分析[J]．力学季刊，2004，**25**(1)：15-20．(YANG Zheng-guang，ZHONG Zheng，DAI Ying．Three dimensional elasticity analysis of a functionally graded rectangular plate[J]．*Chinese Quarterly of Mechanics*，2004，**25**(1)：15-20．(in Chinese))

[3] Celebi K，Yarimpabuc D，Tutuncu N．Free vibration analysis of functionally graded beams using complementary functions method[J]．*Archive of Applied Mechanics*，2018，**88**(5)：729-739．

[4] LI M Z，Guedes Soares C，YAN R J．A novel shear deformation theory for static analysis of functionally graded plates[J]．*Composite Structures*，2020，**250**：112559．

[5] Pandey S，Pradyumna S．Analysis of functionally graded sandwich plates using a higher-order layerwise theory[J]．*Composites Part B：Engineering*，2018，**153**：325-336．

[6] Rezaei A S，Saidi A R，Abrishamdari M，et al．Natural frequencies of functionally graded plates with porosities via a simple four variable plate theory：An analytical approach[J]．*Thin-Walled Structures*，2017，**120**：366-377．

[7] Kumar R，Lal A，Singh B N，et al．New transverse shear deformation theory for bending analysis of FGM plate under patch load[J]．*Composite Structures*，2019，**208**：91-100．

[8] Ferreira A J M，Fasshauer G E．Computation of natural frequencies of shear deformable beams and plates by an RBF-pseudospectral method[J]．*Computer Methods in Applied Mechanics and Engineering*，2006，**196**(1-3)：134-146．

[9] Ferreira A J M，Roque C M C，Martins P A L S．Radial basis functions and higher-order shear deformation theories in the analysis of laminated composite beams and plates[J]．*Composite Structures*，2004，**66**(1-4)：287-293．

[10] Xiang S，Shi H，Wang K M，et al．Thin plate spline radial basis functions for vibration analysis of clamped laminated composite plates[J]．*European Journal of Mechanics - A/Solids*，2010，**29**(5)：844-850．

[11] Ambartsumian S A．On the theory of bending plates[J]．Izv．Otd．Tech．AN．Nauk．SSSR，1958，**5**：69-77．

[12] Aydogdu M．A new shear deformation theory for laminated composite plates[J]．*Composite Structures*，2009，**89**(1)：94-101．

[13] Karama M，Afaq K S，Mistou S．Mechanical behaviour of laminated composite beam by the new multi-layered laminated composite structures model with transverse shear stress continuity[J]．*International Journal of Solids and Structures*，2003，**40**(6)：1525-1546．

[14] Levinson M．An accurate，simple theory of the statics and dynamics of elastic plates[J]．*Mechanics Research Communications*，1980，**7**(6)：343-350．

[15] SHI G Y．A new simple third-order shear deformation theory of plates[J]．*International Journal of Solids and Structures*，2007，**44**(13)：4399-4417．

[16] Soldatos K P，Timarci T．A unified formulation of laminated composite，shear deformable，five-degrees-of-freedom cylindrical shell theories[J]．*Composite Structures*，1993，**25**(1-4)：165-171．

[17] Zenkour A M．Generalized shear deformation theory for bending analysis of functionally graded plates[J]．*Applied Mathematical Modelling*，2006，**30**(1)：67-84．

[18] Guo Q R，Shi G Y．An accurate and efficient 4-noded quadrilateral plate element for free vibration analysis of laminated composite plates using a refined third-order shear deformation plate theory[J]．*Composite Structures*，2023，**324**：117490．

[19] Xiang S，Kang G W．Static analysis of functionally graded plates by the various shear deformation theory[J]．*Composite Structures*，2013，**99**：224-230．

Static analysis of functionally graded plates based on thin plate spline radial basis function

SONG Wei-wei*[1,2,3], XIANG Song[1,2], ZHAO Rui[1,2]

(1. General Aviation Key Laboratory of Liaoning Province, Shenyang Aerospace University, Shenyang 110136, China;
2. Liaoning General Aviation Academy, Shenyang 110136, China;
3. Department of Civil Aviation, Shenyang Aerospace University, Shenyang 110136, China)

Abstract: In this paper, the high-order shear deformation theory is used to model functionally graded plates. The governing differential equations are discretized by a meshless method based on thin plate spline radial basis functions. The calculation results of this article are compared with those of Zenkour et al., and good consistency between the two sets of results indicates the accuracy and effectiveness of the thin plate spline radial basis function method in the analysis of functionally graded plates. It is clear that, the new laminated plate theory proposed in this article that considers the discretization of layer boundaries produces more accurate displacement and stress than other laminated plate theories with five global variables. Numerical examples show that using thin plate spline radial basis functions for static analysis of functionally graded plates has high accuracy and good convergence.

Key words: thin plate spline; radial basis function; functionally graded plates; static analysis; high-order theory; meshless

(上接第 503 页)

Analytical algorithm and influence analysis of sliding cable structure considering friction contact

ZHU Wei-hua*, YAN Dong-huang, XU Hong-sheng

(School of Civil Engineering, Changsha University of Science and Technology, Changsha 410001, Hunan)

Abstract: In order to study the geometric nonlinearity of a sliding cable and the nonlinearity of friction contact between a cable and a pulley, an analytical algorithm for solving the equilibrium state of a sliding cable is proposed. According to the differential equation of equilibrium considering the friction effect between the sliding cable and the pulley, the formulas for calculating the mechanical equilibrium, stress-free length and geometric length of the cable at the pulley are derived. Based on the conservation of stress-free length of the cable, the closure conditions of inter-span height and span, and the mechanical equilibrium condition of the pulley, the nonlinear equations of equilibrium of the sliding cable under its own weight are established. Based on the conservation of stress-free length of a cable segment, the mechanical equilibrium condition of a cable joint, the mechanical equilibrium condition of the pulley, the closure condition of height and horizontal spacing between spans and the conservation principle of stress-free length between adjacent nodes at the pulley, the nonlinear equations of equilibrium of the loaded sliding cable are established. The solution of the equilibrium state is obtained. The results show that the algorithm is a refined algorithm which is closer to the actual engineering situation. The pulley radius and the friction coefficient can be properly adjusted to change the stress-free length and cable force distribution of each cable span.

Key words: sliding cable structure; numerical analytical algorithm; friction contact; catenary theory; nonlinear equations